Original Research

Fluid and White Matter Suppression With the MP2RAGE Sequence

Mark Tanner, BSc,[1] Giulio Gambarota, PhD,[1]* Tobias Kober, PhD,[2,3] Gunnar Krueger, PhD,[2,3] David Erritzoe, MD, PhD,[4] José P. Marques, PhD,[2,5] and Rexford Newbould, PhD[1]

Purpose: To develop a magnetic resonance imaging (MRI) sequence (fluid and white matter suppression, FLAWS) for generating two sets of images from a single acquisition: one with contrast similar to a T1-weighted magnetization-prepared rapid gradient-echo sequence (MPRAGE) for structural definition; the other with nulled white matter (WM) signal intensity, similar to the fast gray matter T1 inversion recovery (FGATIR) sequence, for improved delineation of subcortical brain structures.

Materials and Methods: The recently proposed MP2RAGE, which is a modification of the MPRAGE and generates two image sets at different inversion times, was employed to generate the FGATIR-like contrast (FLAWS1) and MPRAGE-like contrast (FLAWS2). Five healthy volunteers were scanned at 3T and brain tissue contrast and contrast-to-noise were compared.

Results: FLAWS1 and FLAWS2 exhibited similar tissue contrast and contrast-to-noise as the "reference" sequences, FGATIR and MPRAGE, respectively. Synthetic minimum value images generated from FLAWS1 and FLAWS2 provided a gray matter-dominant image.

Conclusion: FLAWS provides two coregistered 3D volumes, one with nulled WM signal intensity and another with nulled cerebrospinal fluid. The coregistered nature of the two datasets allows for generating images that might be helpful in segmentation algorithms and clinical diagnosis.

Key Words: brain; MRI; MPRAGE; brain tissue segmentation; globus pallidus; deep brain stimulation
J. Magn. Reson. Imaging 2012;35:1063–1070.
© 2011 Wiley Periodicals, Inc.

[1]GlaxoSmithKline, Clinical Imaging Center, Imperial College, London, UK.

[2]Laboratory for Functional and Metabolic Imaging, Ecole Polytechnique Fédérale de Lausanne, Lausanne, Switzerland.

[3]Siemens Schweiz AG, Healthcare Sector IM&WS S, Renens, Switzerland.

[4]Department of Clinical Neuroscience, Imperial College, London, UK.

[5]Department of Radiology, University of Lausanne, Lausanne, Switzerland.

*Address reprint requests to: Giulio G., GlaxoSmithKline, Clinical Imaging Center, Imperial College, Du Cane Road, London W12 0NN, UK. E-mail: gambarota@gmail.com

STRUCTURAL MAGNETIC RESONANCE (MR) images of the brain are used for a number of clinical and research applications, which include diagnosis, surgical planning, brain tissue segmentation, and morphometric analysis. A high spatial resolution combined with a high contrast between gray matter (GM) and white matter (WM) and an acquisition time (TA) no longer than 10–15 minutes (1) are often requirements for structural T1-weighted (T1w) images.

Over the last 10 years, and in particular at high magnetic fields of 3T and more, the magnetization-prepared rapid gradient-echo sequence (MPRAGE) has been one of the most commonly used T1w 3D anatomical sequences (2). Today, numerous multicenter trials such as the Alzheimer's Disease Neuroimaging Initiative (ADNI) employ the MPRAGE sequence, due to its superior WM/GM contrast and relatively short scan times (3).

In recent years there has been a growing interest in studying the subcortical brain, which requires robust and precise visualization and delineation of brain structures such as the thalamus, striatum, external and internal globus pallidus (GPe/GPi), red nucleus, and substantia nigra. In particular, precise delineation of such structures is important in a number of clinical/research applications such as deep brain stimulation (DBS). DBS is used in the treatment of involuntary movement disorders in Parkinson's disease or dystonia (4,5). In the case of dystonia, the surgeon aims to use an electrode to stimulate the GPi, although different areas in the basal ganglia and other structures are also targets for treatment of other conditions (4,6,7). Segmentation of these structures based on a T1w image is difficult, due to the low levels of contrast between the basal ganglia and surrounding structures and the absence of easily visible contours (6). To overcome this problem, a number of approaches have been investigated (7–10). Among these, a recent study has proposed a modification of the standard MPRAGE sequence parameters to yield a better visualization of GPe and GPi; this was achieved by using a value of inversion time (TI) shorter (409 msec at 3T) than the TI typically employed in the standard MPRAGE (900 msec at 3T, which nulls the signal of cerebrospinal fluid [CSF]). Shortening of the TI resulted in nulling the signal of WM while preserving most of

the signal of GM and CSF (7). As a consequence, images acquired with this modified version of MPRAGE (fast gray matter T1 inversion recovery, FGATIR) displayed a sharper delineation of GPe and GPi when compared with conventional MPRAGE, and revealed interesting features such as the internal lamina of the GPi, fiber bundles from the internal capsule piercing the striatum, and the boundaries of the subthalamic nucleus (7).

Recently, a new sequence has been developed to create T1w images and estimate T1-maps in the presence of inhomogeneous reception and transmission (B_1) fields (11). The sequence, MP2RAGE, is a variation of the standard MPRAGE sequence where, following the inversion of the longitudinal magnetization, two images are acquired with a radiofrequency (RF)-spoiled rapid gradient echo readout train at each of two different inversion times. In the MP2RAGE study (11), the inversion times, repetition time, and flip angles were optimized in order to create a synthetic image with optimum contrast between brain tissues. The created synthetic MP2RAGE image is free of proton density and T2* contrast, reception bias field, and (to a large extent) transmit field inhomogeneity and can be therefore used to calculate T1 values.

Motivated by the need to acquire T1w structural images as well as images that provide good visualization of subcortical structures such as GPe/GPi, we aimed to generate both contrasts, that is, an "MPRAGE-like" contrast and an "FGATIR-like" contrast in a single scan. This single-scan approach would also have the advantage that the two images are perfectly registered with each other.

In the current study we exploited the attractive feature of the MP2RAGE sequence of generating two inherently coregistered images with different contrasts. The MP2RAGE sequence parameters were optimized via Bloch simulations in order to create two images with properties comparable to the FGATIR and MPRAGE, respectively. The images obtained with "fluid and white matter suppression" (FLAWS) were compared with the conventional MPRAGE and FGATIR protocols in five healthy volunteers.

MATERIALS AND METHODS
FLAWS Optimization

Bloch simulations of the signal behavior throughout the MP2RAGE sequence (11) were performed to optimize FLAWS sequence parameters. The goal of the optimization was to achieve a good suppression of WM in one image ("FGATIR-like") and of CSF in the other image ("MPRAGE-like"), yet maintaining a good contrast for the basal ganglia structures. The MP2RAGE sequence consists of an adiabatic inversion pulse, followed by two gradient-echo (GRE) readout modules that sample the longitudinal magnetization, to generate two images at two different inversion time (TI) points (TI_1 and TI_2) of the T1 recovery curve. In the Bloch simulations, the relevant sequence parameters were the following: the MP2RAGE repetition time (TR, range 3–9 sec), which is the time interval between two consecutive

Table 1
Sequence Parameters for FGATIR, ADNI-MPRAGE, and FLAWS

	FGATIR	ADNI-MPRAGE	FLAWS (TI_1,TI_2)
TR/TE (msec)	3000/2.96	2300/2.98	5000/2.94
TI (msec)	409	900	409, 1100
Flip angle	8°	9°	5°, 5°
Matrix	240x256	240x256	240x256
Slices	160x1mm	160x1mm	160x1mm
BW (Hz/px)	240	240	240
Orientation	Sagittal	Sagittal	Sagittal
FOV (mm)	240/256	240/256	240/256
iPAT	1	1	2
Slice partial Fourier	6/8	Off	6/8
Scan time	12:02	09:14	10:57

inversion pulses, the repetition time of the GRE modules (TR_{GRE}, range 4–10 msec), the flip angles of the GRE modules (α_1 and α_2, range 2°–12°), the number of excitations per GRE module (range 120–200), and the inversion times TI_1 (200–500 msec) and TI_2 (700–1300 msec). In the simulations, the efficiency of the inversion adiabatic pulse was assumed to be ideal and literature values of T_1 of WM (0.81 sec), GM (1.35 sec), and CSF (2.5 sec) at 3T were used (11).

MRI

MRI experiments were performed at 3T (Magnetom Verio, Siemens Healthcare Sector, Erlangen, Germany) with a 32-receiver channel head matrix coil. The ADNI-recommended MPRAGE protocol was used as a reference to dictate a number of parameters, which included a sagittal orientation, and 240 Hz/Px bandwidth. Throughout the article we refer to the ADNI-recommended MPRAGE acquisition as simply MPRAGE. Other sequence parameters, for both the MPRAGE and FGATIR, were similar to those given in the respective article (Table 1). All three sequences used a 1 mm^3 voxel size, anteroposterior phase-encoding direction, and a symmetric echo. FLAWS used a nonselective hyperbolic secant inversion pulse of 10.24 msec duration and nonselective rectangular excitation pulses of 0.1 msec duration. The duration between two adjacent excitation pulses was 6 msec. In all three sequences the TI was defined from the start of the inversion pulse to the acquisition of the center of k-space by each GRE module, which transversed k-space linearly.

In addition, FGATIR and FLAWS required 6/8 slice partial Fourier to enable the value of the short inversion time (TI_1). The output of the FLAWS sequence consisted of two sets of images: the 3D volume acquired at TI_1 (FLAWS1) and that acquired at TI_2 (FLAWS2). Five healthy subjects took part in the study (three males, two females, age 31–45). Subjects were scanned on one study visit, using the MPRAGE, FGATIR, and FLAWS sequences. In addition to the data from the five volunteers, an incidental finding in a volunteer with a history of intermittent excessive alcohol consumption—from a study where the FLAWS sequence was employed—is shown in the Results section. All
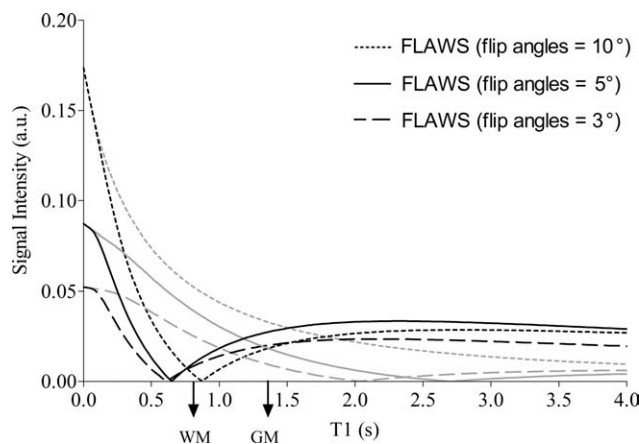
Figure 1. Simulated signal intensity of FLAWS1 (black lines) and FLAWS2 (gray lines) as a function of the tissue T1 for different flip angles (10°, dotted line; 5°, continuous line; 3°, dashed line). The T1 of WM and GM at 3T is indicated by the arrow.

experiments were conducted according to the procedures approved by the Institutional Review Board.

Data Analysis

Data analysis was performed on the four 3D volumes (MPRAGE, FGATIR, FLAWS1, and FLAWS2) using ImageJ (12). Regions of interest (ROIs) were manually drawn on the MPRAGE image in a central brain location, specifically in the corpus callosum (splenium) for WM (80 mm³), caudate nucleus (head) for GM (69 mm³), and lateral ventricle (body) for CSF (112 mm³). The size of ROIs was the same for all five datasets. As a result, the three ROIs were at a similar distance from the receiver coils. The contrast (CN) and contrast-to-noise ratio (CNR) were calculated for WM/GM, GM/CSF, and CSF/WM according to the equations $CN = (S_a - S_b)/(S_a + S_b)$ and $CNR = (S_a - S_b)/(\sqrt{((SD_a^2 + SD_b^2)/2)})$, where S_a (S_b) is the mean signal intensity and SD_a (SD_b) is the standard deviation of tissue a (b) within the ROI (13). In order to remove any bias when comparing sequences with different parallel imaging factors, this formula for CNR was preferred over the more common equation that uses the standard deviation of the signal intensity of an ROI in air. Statistical analysis was performed using GraphPad Prism v. 3.0 (GraphPad Software, La Jolla, CA). Furthermore, synthetic images were generated from the FLAWS scan by taking the minimum pixel value from the perfectly registered FLAWS1 and FLAWS2 contrasts in order to enhance specific tissue contrast.

RESULTS

An illustrative example of the effect of flip angles (α_1 and α_2) on the signal intensity of FLAWS1 and FLAWS2, as a function of the tissue T1, is shown in Fig. 1. The other sequence parameters are identical to those in Table 1. The simulated signal intensity of FLAWS1 (black lines) displays a sharp minimum, with the position of the minimum highly sensitive to the

value of the flip angles. In FLAWS1, the signal intensity of GM for (α_1, α_2) of (5°, 5°, continuous line) is higher than that for (α_1, α_2) of (3°, 3°, dashed line) and (10°, 10°, dotted line). The simulated signal intensity of FLAWS2 (gray lines) is overall monotonically decreasing with the T1 of tissues. Minor deviations from monotonic behavior are observed for flip angles (α_1 and α_2) of (3°, 3°) and (5°, 5°) at T1 > 2 seconds. Overall, excellent CSF suppression is achieved with the flip angles of (3°, 3°) and (5°, 5°) in FLAWS2. A similar subset of the full Bloch simulation space is presented in Fig. 2 for inversion times. Small changes of the inversion times (TI₁, TI₂) have a substantial effect on the null point of the signal intensity of FLAWS1 (ie, on WM suppression) but only a minor effect on the signal intensity of FLAWS2.

Sagittal head images obtained with MPRAGE, FGA-TIR, and FLAWS (FLAWS1 and FLAWS2) are shown in Fig. 3. Overall, FLAWS2 (Fig. 3c) yields tissue contrast comparable to the MPRAGE (Fig. 3a), with nulled CSF, intermediate GM, and bright WM signal intensity. Similarly, FLAWS1 (Fig. 3d) produces an FGA-TIR-like contrast (Fig. 3b), with low signal intensity of WM and intermediate signal intensity of GM; higher CSF signal is noticeable in FLAWS1 when compared with FGATIR. Good delineation of structures such as the mammillothalamic tract (Fig. 4a,b), the GPe/GPi and the internal lamina (Fig. 4c,d), and the substantia nigra (Fig. 4e, f), is noticeable in the FGATIR (top row) and FLAWS1 (bottom row) images. Comparable subcortical contrast and image quality is also observed between FLAWS1 and FGATIR.

The quantitative measurements of CN and CNR for WM/GM, GM/CSF, and CSF/WM in FLAWS1, FLAWS2, FGATIR, and MPRAGE are given in Tables 2 and 3. FLAWS2 shows similar CNR for WM/GM, GM/CSF, and CSF/WM as the MPRAGE (Table 2). FLAWS2 and MPRAGE are also characterized by similar WM/GM contrast; on the other hand, improved contrast for WM/CSF ($P = 0.012$) and GM/CSF ($P = 0.010$) is observable in FLAWS2 (Table 2).
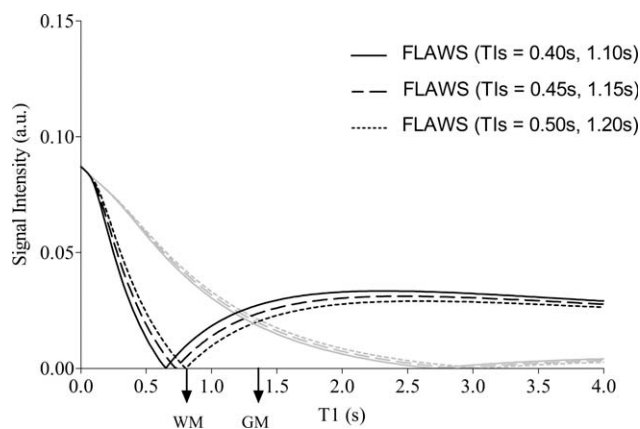

Figure 2. Simulated signal intensity of FLAWS1 (black lines) and FLAWS2 (gray lines) as a function of the tissue T1 for different inversion times (TI₁, TI₂ = 0.40 sec, 1.10 sec, continuous line; 0.45 sec, 1.15 sec, dashed line; 0.50 sec, 1.20 sec, dotted line). The T1 of WM and GM at 3 T is indicated by the arrow.
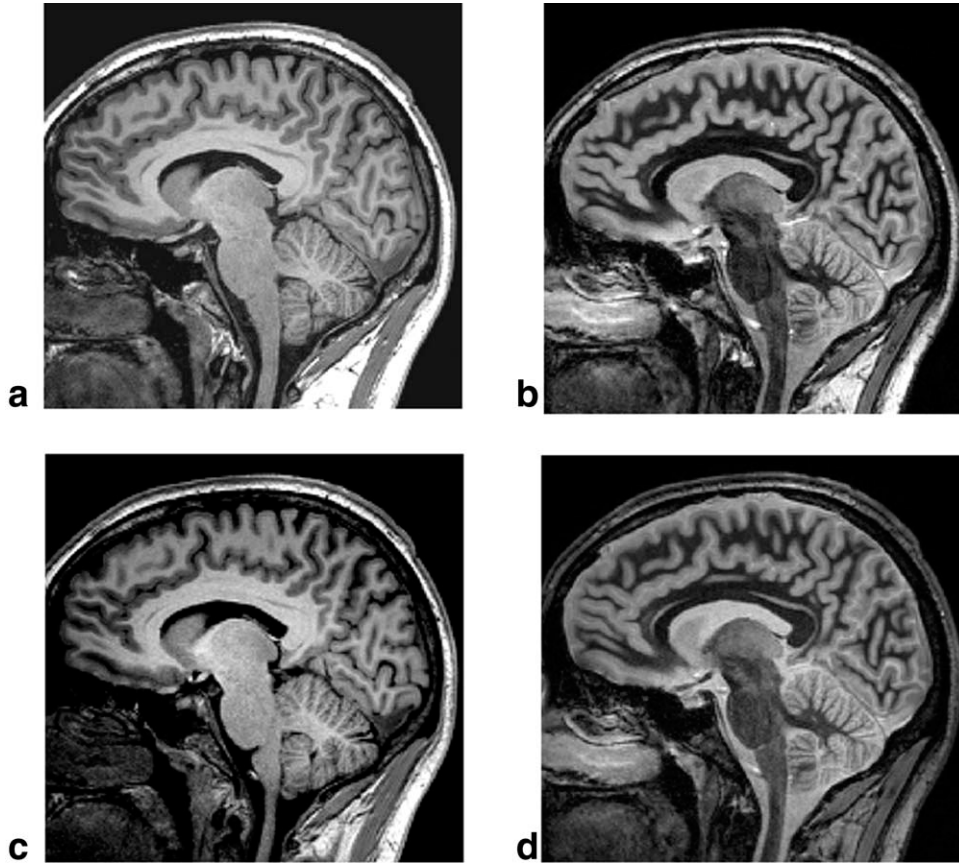
Figure 3. Sagittal brain MR images of a healthy volunteer acquired with MPRAGE **(a)**, FGATIR **(b)**, and FLAWS (second inversion time, TI_2 = 1100 msec, FLAWS2 **(c)**, and first inversion time, TI_1 = 409 msec, FLAWS1 **(d)**). Brain tissue contrast in FLAWS1 and FLAWS2 is comparable to that of FGATIR and MPRAGE, respectively.
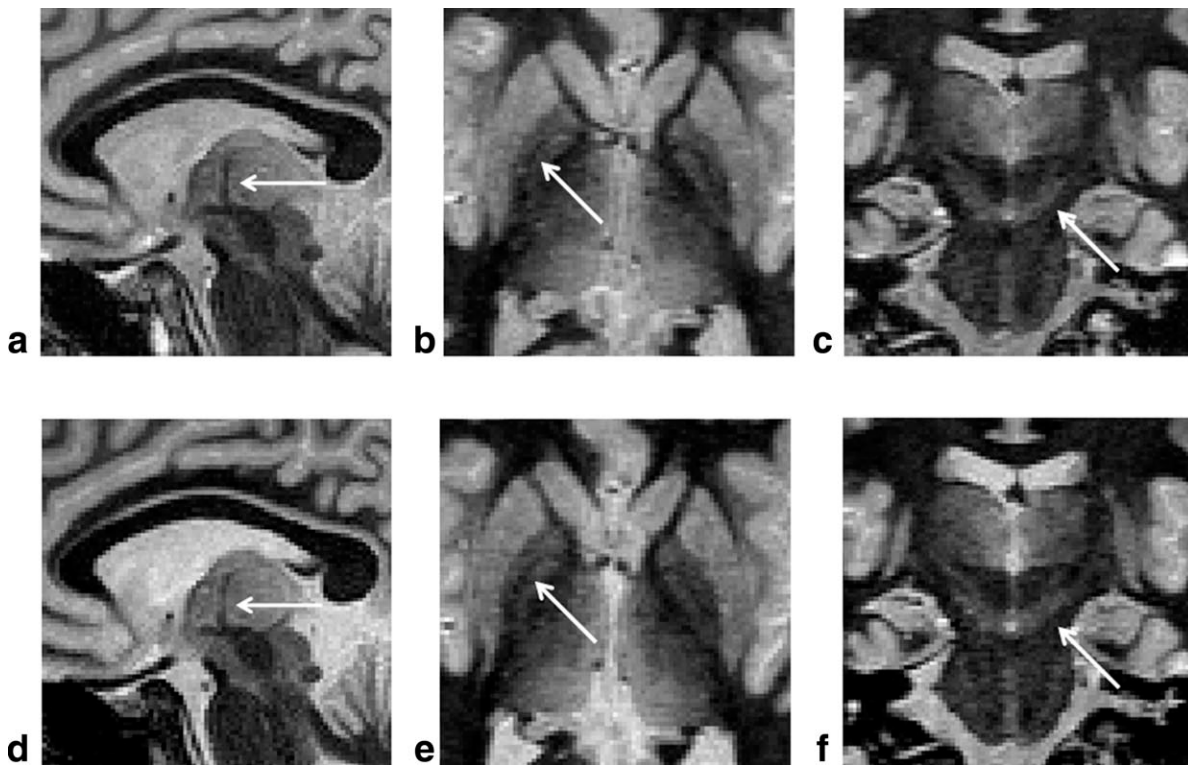

Figure 4. Brain MR images of a healthy volunteer acquired with FGATIR (top) and FLAWS (first inversion contrast, FLAWS1, bottom). FGATIR and FLAWS yield comparable contrast and delineation of the mammillothalamic tract **(a,d)**, globus pallidus **(b,e)**, where the white arrow depicts the subdivision in external and internal globus pallidus, and the substantia nigra **(c,f)**, respectively.

Table 2
Mean Contrast (CN) and Contrast-to-Noise Ratio (CNR) Values for WM, GM, and CSF in MPRAGE and FLAWS2 ($n = 5$)

| Tissue | Calculation | Sequence | | P |
		MPRAGE	FLAWS2	
WM/GM	CNR	5.74 (4.31-7.43)	5.33 (4.58-6.52)	0.565
	CN	0.14 (0.11-0.16)	0.15 (0.13-0.16)	0.365
WM/CSF	CNR	19.41 (16.04-22.42)	21.36 (14.26-26.57)	0.306
	CN	0.67 (0.64-0.70)	0.83 (0.68-0.89)	0.012
GM/CSF	CNR	12.19 (10.76-13.14)	15.25 (10.18-17.86)	0.116
	CN	0.58 (0.57-0.61)	0.78 (0.60-0.86)	0.010

P values describe two-tailed paired *t*-test between MPRAGE and FLAWS2. Ranges of CN and CNR values are in parentheses.

FGATIR displays higher contrast than FLAWS1 between WM/GM and WM/CSF ($P < 0.001$ in both cases), although lower contrast between GM/CSF ($P = 0.002$). FLAWS1 has better CNR than FGATIR between GM/CSF ($P = 0.003$), whereas improved CNR for WM/GM ($P = 0.069$) is observable in FGATIR. FGATIR has better CNR than FLAWS1 between GM/CSF ($P = 0.002$). FLAWS1 and FGATIR share virtually the same CNR for WM/CSF ($P = 0.998$).

Figure 5 shows sagittal, axial, and coronal minimum images, generated by taking the minimum pixel value of FLAWS1 and FLAWS2. Since WM and CSF are hypointense versus GM in FLAWS1 and FLAWS2, respectively, the minimum image represent predominantly GM as well as tissues of similar T1 value as GM. An example of the benefits of the additional contrast provided by FLAWS and the minimum image is shown in Fig. 6. WM lesions, observed as an incidental finding in a subject other than the five healthy volunteers, are shown in axial (Fig. 6, top row) and sagittal (Fig. 6, bottom row) planes in FLAWS1 (Fig. 6a,b), FLAWS2 (Fig. 6c,d), and minimum images (Fig. 6e,f). The WM lesion, as well as the adjacent CSF, is hyperintense in FLAWS1 and displays a high contrast with the surrounding to normal-appearing WM. The inverse signal contrast is observed in FLAWS2. The calculated minimum image provides hypointense WM and CSF, enhancing lesion contrast by demarcating the ventricular margins.

DISCUSSION

In the current study we propose an MRI sequence, FLAWS, that in a single scan provides a coregistered set of two 3D images, one with a nulled WM signal intensity and another with nulled CSF. The early contrast, achieved with a TI of ≈400 msec, yields visual-ization of basal ganglia structures, and is similar to the contrast of the FGATIR sequence. The late contrast, from a TI of ≈1 second, is similar to the MPRAGE contrast, and it is of interest for displaying general brain anatomy and structural segmentation. FLAWS is a modification of the recently proposed MP2RAGE sequence, which allows for the acquisition of two sets of images at two different timepoints of the T1 recovery curve, following adiabatic inversion of the magnetization. As such, the contrast achievable in FLAWS, and other potential variants of MP2RAGE, is dictated by the T1 relaxation time of the tissues and can be manipulated primarily by changing the values of inversion times, but also via excitation flip angles and TR times. It would be possible to generate other contrasts, such as nulling GM, by varying these parameters.

Quantitative analysis of tissue contrast showed that, overall, the "FGATIR-like" contrast of FLAWS1 and "MPRAGE-like" contrast of FLAWS2 have CNR and CN better or comparable to that of FGATIR and MPRAGE, respectively, with the exception of WM/GM and WM/CSF contrast of FGATIR. It should be noted that the better WM/GM and WM/CSF contrast of FGATIR vs. FLAWS1 is related to the degree of WM signal intensity nulling. In preliminary experiments it was observed that it was feasible, by careful optimization of the first TI with Bloch simulations, to achieve a better WM signal suppression in FLAWS1 than that achieved with the parameters of Table 1. For instance, with the first TI value of 0.5 seconds (Fig. 2) excellent WM suppression was achieved in vivo (data not shown); however, this resulted in poor discrimination of basal ganglia structures, especially the globus pallidus (GP). The GP has a T1 relaxation time closer to WM than GM (T1$_{WM}$ = 0.81 ± 0.03 sec; T1$_{GM}$ = 1.35 ± 0.05 sec; T1$_{GP}$ = 0.97 ± 0.07 sec (11)) so the more complete nulling of WM resulted in a loss of signal

Table 3
Mean Contrast (CN) and Contrast-to-Noise Ratio (CNR) Values for WM, GM, and CSF in FGATIR and FLAWS1 ($n = 5$)

| Tissue | Calculation | Sequence | | P |
		FGATIR	FLAWS1	
WM/GM	CNR	13.20 (10.58-15.29)	11.61 (9.72-12.77)	0.069
	CN	0.76 (0.65-0.87)	0.59 (0.51-0.69)	< 0.001
WM/CSF	CNR	16.69 (15.82-18.59)	16.68 (14.45-18.36)	0.998
	CN	0.79 (0.70-0.88)	0.68 (0.62-0.77)	< 0.001
GM/CSF	CNR	2.37 (1.22-3.14)	5.72 (4.81-6.42)	0.003
	CN	0.08 (0.04-0.10)	0.16 (0.13-0.17)	0.002

P values describe two-tailed paired *t*-test between FGATIR and FLAWS1. Ranges of CN and CNR values are in parentheses.
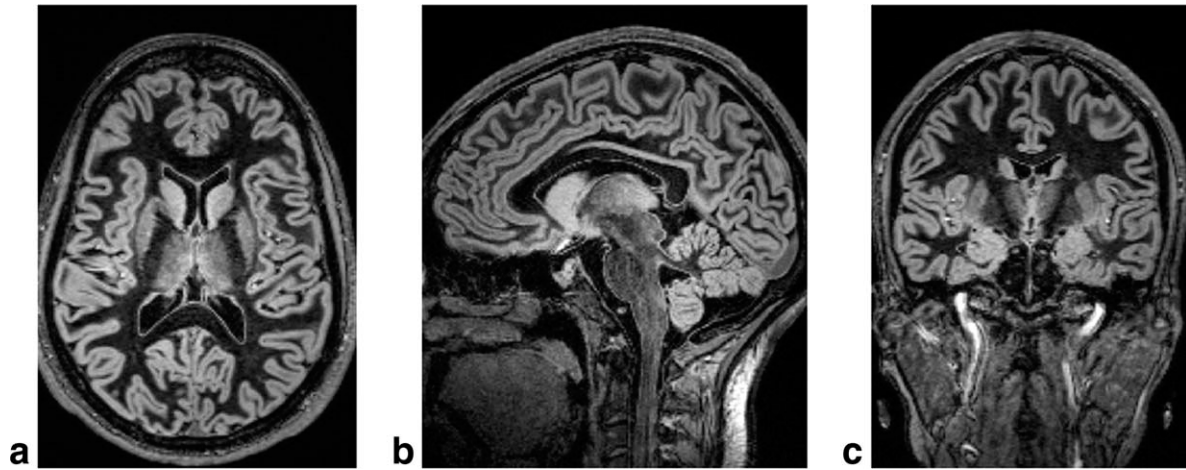
Figure 5. Minimum value brain MR images of a healthy volunteer in axial **(a)**, sagittal **(b)**, and coronal planes **(c)**. Images were generated by taking the minimum pixel value between FLAWS1 and FLAWS2. Since WM and CSF are hypointense in FLAWS1 and FLAWS2, respectively, the signal intensity of the minimum image is predominantly GM.

from the GP and other tissues with T1 similar to WM. Thus, in the final protocol (Table 1) the first TI was chosen so to provide a compromise between WM nulling and visualization of basal ganglia structures, in order to obtain an contrast and overall quality image comparable with FGATIR.

The longer TR that is required in FLAWS (compared with MPRAGE and FGATIR) to acquire two datasets of images at two TIs—as well as to allow for a sufficient T1 recovery of the magnetization—results in an increased imaging time that makes FLAWS less prac-

tical in clinical settings unless parallel imaging is employed. It is well documented that using parallel imaging has the effect of creating variable spatial signal-to-noise ratio (SNR), being particularly worse in the center of the image (14). However, Wonderlick et al (15) discussed that, with conservative parallel imaging factors, there is a "negligible effect on reliability of morphometric measures" when examining the MPRAGE sequence. In addition, with respect to SNR, it should be noted that the use of highly sensitive coils, such as the 32-channel coil employed in the
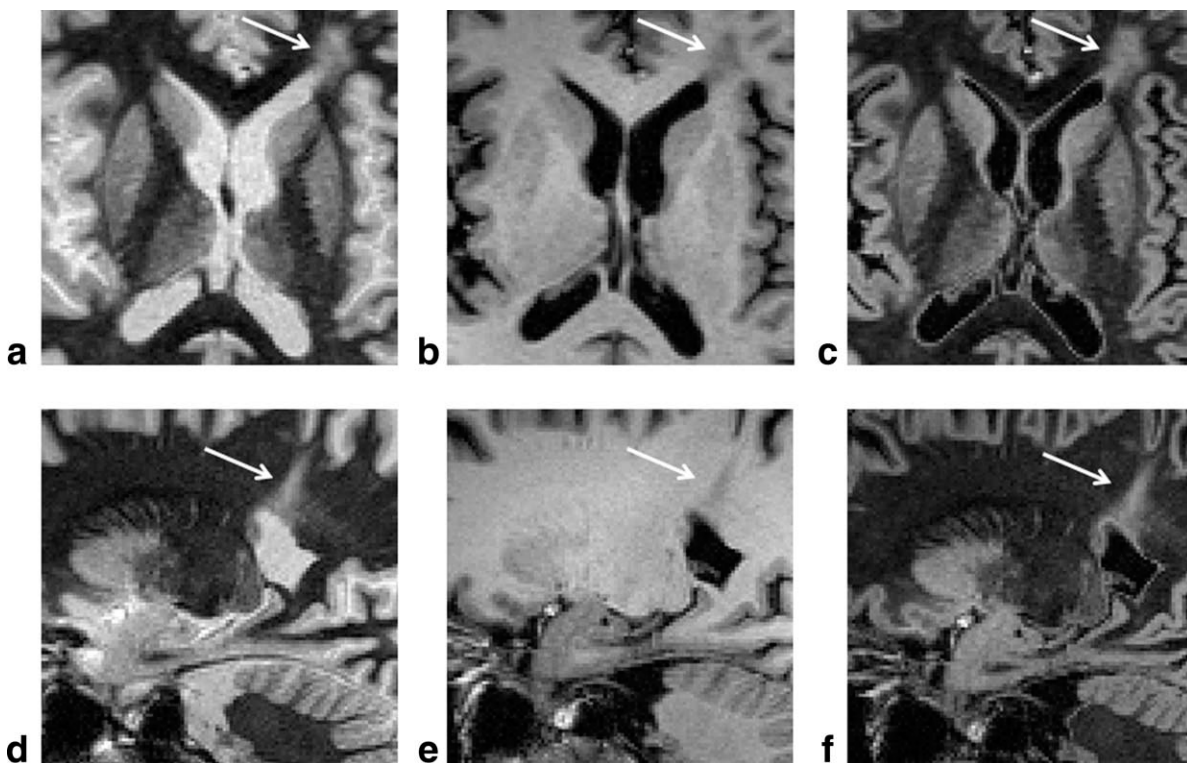

Figure 6. Axial (top) and sagittal (bottom) brain MR images displaying WM pathology in FLAWS1 **(a,d)**, FLAWS2 **(b,e)**, and calculated minimum image **(c,f)**. This demonstrates that the minimum image may help to highlight pathology, especially WM periventricular pathology.

current study, is important to obtain good image quality with the FLAWS parameters proposed.

FLAWS, as a modification of the MP2RAGE, allows for acquisition of both contrasts in a single scan; this has the advantage that the two datasets are perfectly registered with each other. As a result, it is possible to easily combine the two contrasts and generate images that provide tissue-specific enhancement. For instance, the minimum image generated from the two contrasts is characterized by nulled CSF and WM signal intensity (see Fig. 5), with a close resemblance to the contrast of the double inversion recovery sequence (16,17) which results in low CSF and WM signal intensity. This calculated minimum image gives a GM-specific image and has the ability of enhancing the visualization of WM lesions (see Fig. 6). GM images could be also generated by using the synthesizing algorithm proposed in the original MP2RAGE article (11); this algorithm has the advantage of reducing B_1 inhomogeneity. On the other hand, GM images generated with the minimum image approach retain some of the T2* contrast that allows for better discrimination of red nucleus, substantia nigra, and globus pallidus. In general, the additional contrast and the possibility of combining images could be useful in brain tumor imaging and other neuropathologies.

A second advantage of the coregistered datasets is the ability to leverage the large suites of neuroimaging tools developed to exploit the ADNI-recommended MPRAGE contrasts. Operations such as brain extraction, spatial normalization, motion correction, and segmentation may be calibrated using the second (MPRAGE-like) FLAWS images, and then applied on the higher WM/GM contrast FLAWS1 images.

In recent years there has been a growing interest in delineation of subcortical brain structures for a number of clinical/research applications. One clinical example for such a need is DBS. The imaging mainstay is a stereotactic 3D-T1 weighted gradient echo MR acquisition, such as MPRAGE. This is often used in combination with 2D fast spin-echo (FSE) inversion recovery (IR), 2D FSE T2-weighted sequences in multiple planes, and in some cases contrast-enhanced sequences (4,18). In a recent study a modification of MPRAGE, FGATIR, was proposed to improve visualization of subcortical structures (7). FLAWS could be advantageous in DBS imaging, as it provides a traditional T1-like contrast—that the surgeon is familiar with—and FGATIR-like high contrast deep brain structure delineation in one 3D acquisition, and may remove the need to acquire other 2D sequences in multiple planes.

FLAWS could further be useful in positron emission tomography (PET) brain studies where delineation of the dopamine-rich structures is necessary. Tziortzi et al (19) described a method for defining various structures rich in dopamine receptors using a T1w MRI sequence. However, due to the inability to visualize the SN clearly on the 3D-T1w images, it was necessary to use the lower-resolution PET images with its inherent potential partial volume effects to help delineation of the SN. As shown in the current study, the SN can be seen on both FLAWS1 and FGATIR (Fig.

4e,f). Tziortzi et al also commented that a further limitation of using 3D-T1w images was their inability to subdivide certain areas; for instance, it was not possible to depict both the GPi and GPe. Again, this subdivision can be identified in both FGATIR and FLAWS1 (see Fig. 4c,d).

It should be noted that, in addition to the study of FGATIR (7), many others have explored techniques for contrast enhancement of subcortical structures. Examples include magnetization transfer imaging (8), T1 and T2* maps (9), and susceptibility weighted imaging (10). Some are characterized by long imaging times and/or multiple acquisitions that require consistent head position, which could be difficult to translate into clinical settings. Overall, the major advantage of FLAWS over previously proposed methods is the ability to provide, in a reasonable acquisition time (<11 min), a coregistered set of two volumes as well as images that provide good visualization of basal ganglia structures.

In conclusion, FLAWS provides comparable CNR against the respective "reference" sequences, MPRAGE and FGATIR. FLAWS can be acquired in a reasonable time and can produce two useful contrasts for little time detriment from the conventional MPRAGE. The feature of acquiring two image datasets with different inversion times within the same sequence and head geometry gives the opportunity to create calculated images harnessing specific tissue contrasts, which might be helpful in segmentation algorithms and clinical diagnosis.

REFERENCES

1. Deichmann R, Good CD, Josephs O, Ashburner J, Turner R. Optimization of 3-D MP-RAGE sequences for structural brain imaging. NeuroImage 2000;12:112–127.
2. Mugler J, Brookeman J. Three-dimensional magnetization-prepared rapid gradient-echo imaging (3D MP-RAGE). Magn Reson Med 1990;15:152–157.
3. Jack CR Jr, Bernstein MA, Fox NC, et al. The Alzheimer's Disease Neuroimaging Initiative (ADNI): MRI methods. J Magn Reson Imaging. JMRI 2008;27:685–691.
4. Pinsker MO, Volkmann J, Falk D, et al. Deep brain stimulation of the internal globus pallidus in dystonia: target localisation under general anaesthesia. Acta Neurochir (Wien) 2009;151:751–758.
5. Wider C, Pollo C, Bloch J, Burkhard PR, Vingerhoets FJ. Long-term outcome of 50 consecutive Parkinson's disease patients treated with subthalamic deep brain stimulation. Parkinsonism Relat Disord 2008;14:114–119.
6. Vasques X, Cif L, Hess O, Gavarini S, Mennessier G, Coubes P. Stereotactic model of the electrical distribution within the internal globus pallidus during deep brain stimulation. J Comput Neurosci 2009;26:109–118.
7. Sudhyadhom A, Haq IU, Foote KD, Okun MS, Bova FJ. A high resolution and high contrast MRI for differentiation of subcortical structures for DBS targeting: the fast gray matter acquisition T1 inversion recovery (FGATIR). NeuroImage 2009;47(Suppl 2):T44–52.
8. Helms G, Draganski B, Frackowiak R, Ashburner J, Weiskopf N. Improved segmentation of deep brain grey matter structures using magnetization transfer (MT) parameter maps. NeuroImage 2009;47:194–198.
9. Baudrexel S, Nurnberger L, Rub U, et al. Quantitative mapping of T1 and T2* discloses nigral and brainstem pathology in early Parkinson's disease. NeuroImage 2010;51:512–520.
10. Abosch A, Yacoub E, Ugurbil K, Harel N. An assessment of current brain targets for deep brain stimulation surgery with susceptibility-weighted imaging at 7 Tesla. Neurosurgery 2010;67:1745–1756; discussion 1756.

11. Marques JP, Kober T, Krueger G, van der Zwaag W, Van de Moortele PF, Gruetter R. MP2RAGE, a self bias-field corrected sequence for improved segmentation and T1-mapping at high field. NeuroImage 2010;49:1271–1281.

12. Abramoff MD, Magelhaes PJ, Ram SJ. Image processing with ImageJ. Biophoton Int 2004;11:36–42.

13. Lee JN, Riederer SJ. The contrast-to-noise in relaxation time, synthetic, and weighted-sum MR images. Magn Reson Med 1987; 5:13–22.

14. Lindholm TL, Botes L, Engman EL, et al. Parallel imaging: is GRAPPA a useful acquisition tool for MR imaging intended for volumetric brain analysis? BMC Med Imaging 2009;9:15.

15. Wonderlick JS, Ziegler DA, Hosseini-Varnamkhasti P, et al. Reliability of MRI-derived cortical and subcortical morphometric measures: effects of pulse sequence, voxel geometry, and parallel imaging. NeuroImage 2009;44:1324–1333.

16. Redpath TW, Smith FW. Technical note: use of a double inversion recovery pulse sequence to image selectively grey or white brain matter. Br J Radiol 1994;67:1258–1263.

17. Wattjes MP, Lutterbey GG, Gieseke J, et al. Double inversion recovery brain imaging at 3T: diagnostic value in the detection of multiple sclerosis lesions. AJNR Am J Neuroradiol 2007;28:54–59.

18. Pollo C, Vingerhoets F, Pralong E, et al. Localization of electrodes in the subthalamic nucleus on magnetic resonance imaging. J Neurosurg 2007;106:36–44.

19. Tziortzi AC, Searle GE, Tzimopoulou S, et al. Imaging dopamine receptors in humans with [11C]-(+)-PHNO: dissection of D3 signal and anatomy. NeuroImage 2011;54:264–277.